JOURNAL OF MATERIALS SCIENCE 33 (1998) 3371–3376

Dissolution and adhesion behaviour of radio-frequency magnetron-sputtered Ca–P coatings

J. G. C. WOLKE*‡, K. DE GROOT*, J. A. JANSEN‡
*Department of Biomaterials, University of Leiden, Prof. Bronckhorstlaan 10, 3723 MB Bilthoven, The Netherlands
‡Unit Oral Function, Department of Biomaterials, University of Nijmegen, Dental School, PO Box 9101, 6500 HB Nijmegen, The Netherlands

Radio-frequency magnetron sputtering deposition was used to produce calcium phosphate sputter coatings with three different thicknesses (0.1, 1 and 4 μm) on titanium discs. Half of the as-sputtered coatings were subjected to an additional heat treatment for 2 h at 500 °C. X-ray diffraction demonstrated that annealing at 500 °C changed the amorphous 1 and 4 μm sputtered coatings into an amorphous–crystalline structure, while the amorphous 0.1 μm changed in a crystalline apatite structure. Further, scanning electron microscopy (SEM) inspection demonstrated that annealing of the 1 and 4 μm coatings resulted in the appearance of some cracks. The dissolution behaviour of these Ca–P coatings was determined in a simulated body fluid. It was found that after incubation for 4 weeks the dissolution was determined by the crystallinity of the deposited coating. SEM and Fourier transform infrared evaluation showed that all the heat-treated sputter coating appeared to be stable under the test conditions and a Ca–P precipitate was always deposited on the coating surface. On the other hand, the amorphous 0.1 and 1 μm coatings dissolved completely within 4 weeks, while the amorphous 4 μm coating showed only signs of surface dissolution. Scratch testing demonstrated that there is a linear correlation between the critical load, L_c, and the coating thickness. A heat treatment for the CaP-4 coating resulted in an additional decrease in the critical load. On the basis of these findings, we conclude that already a 0.1 μm heat-treated Ca-P sputter coating is of sufficient thickness to show *in-vitro* adequate bioactive and adhesive properties.

1. Introduction

The recent concerns that have been raised about the clinical feasibility of plasma-sprayed Ca–P coatings deal with the accelerated dissolution and/or delamination of these coatings [1–4]. To solve these problems, we suggested the use of a radio-frequency (RF) magnetron sputtering technique to deposit Ca–P coatings [5]. Previous results in our laboratory showed that the deposited films had a uniform and dense structure, especially on complex implant materials. Further the dissolution of the coatings in Gomori's buffer appeared to be partly determined by the crystallinity of the deposited coating. Amorphous sputtered coating dissolved completely within 4 weeks, while the dissolution rate of the crystalline-sputtered and heat-treated films was much lower [6, 7].

On the other hand, we also know that dissolution studies in Gomori's buffer are not predictive for the final chemical behaviour of Ca–P coatings [8, 9]. This is confirmed by a study in which we inserted amorphous and crystalline Ca–P sputter-coated discs into the back of rabbits [10]. Although the amorphous coatings dissolved within 4 weeks, this was followed by the precipitation of carbonate apatite. Therefore, some researchers claim that the use of physiological media is essential to investigate the preclinical dissolution behaviour of Ca–P films [11].

Besides the above mentioned we also know that the final effectiveness of our sputtered Ca–P coating will depend strongly on the degree of adhesion between coating and its underlying substrate. The adhesion strength of a coating is considered to be the amount of energy which is required to separate it from the substrate. However, this energy is very difficult to measure. Many methods for detaching coatings have already been developed. Although some of these are very sophisticated, such as the laser spallation [12] and the Lorentz force method [13], they are not really of routine practical use. More conventional methods are Scotch tape tests, pull-off method, three- or four-point bending tests, indentation tests and scratch tests [14–16]. The maximum adhesion that can be tested by the Scotch tape and pull-off method is less than the strength of the used tape and adhesive. Both methods are limited to relative thick films with poor adhesion to the substrate. To obtain information about the adhesion strength of thin sputtered Ca–P coatings indentation, bending and scratch adhesion methods appear to be the most accessible approach. Therefore, the aim of this study was to investigate the dissolution

0022–2461

behaviour of various calcium phosphate magnetron-sputtered coatings in simulated body fluid (SBF). The adhesion strengths of these coatings were studied by the means of scratch tests.

2. Materials and methods

2.1. Ca–P sputter coatings

For the experiments, commercially pure titanium discs were provided with Ca–P sputter coatings. The discs were cut from commercially pure titanium rods with a diameter of 12 mm and a thickness of 1 mm. The coatings were deposited using a commercially available RF magnetron sputter unit (Edwards ESM 100). The target material used in the deposition process was a copper disc provided with a plasma-sprayed hydroxyapatite (HA) coating (CAM®). The process pressure was 5×10^{-3} mbar and the sputter power was 400 W. The deposition rate of the films was 100–150 nm min^{-1} sputtering. Coatings with three different thicknesses were prepared. CaP-0.1, thickness of 0.1 μm; CaP-1, thickness of 1 μm; CaP-4, thickness of 4 μm Half the specimens were subjected to an additional heat treatment for 2 h at 500 °C.

Before and after annealing, coatings were characterized.

(a) The crystallographic structure of each film was determined by X-ray diffraction (XRD) using a Philips vertical θ–2θ diffractometer and a Philips horizontal diffractometer, rebuilt as a thin-film diffractometer using a Cu Kα radiation.

(b) The infrared spectra of the films on the substrates were obtained by reflection Fourier transform infrared (FITR) spectroscopy (Perkin–Elmer).

(c) The surface topology of the films was examined using scanning electron microscopy (SEM).

(d) The elemental composition of the films was determined with energy-dispersive spectroscopy (EDS).

These analyses showed that the as-deposited coating had an amorphous structure and that heat treatment resulted in an amorphous–crystalline apatite structure for the CaP-1 and CaP-4 coatings, while the heat-treated CaP-0.1 coatings had a well-crystallized structure with hardly no amorphous phase. Further, annealing of the CaP-1 and CaP-4 coatings resulted in the appearance of some cracks. This phenomena could not be confirmed for the CaP-0.1 coating, owing to its very small thickness. The elemental composition of the coatings showed that the Ca-to-P ratio varied between 1.8 and 2.0.

2.2. Dissolution assay

All coated specimens were incubated in 4 ml of SBF buffer with a pH of 7.2 at 37 °C (Table I) [17] for 4 weeks. The experiment was performed in triplicate. At time periods of 1, 2, 3 and 4 weeks, the SBF buffer solution was refreshed. For each sample, the Ca and P concentrations in the solutions were determined in triplicate by flame atomic absorption spectrometry (Varian model AAS 300) and spectrophotometry (Vitatron), respectively. At the end of the experiment, coated samples were retrieved from the SBF solution.

TABLE I Composition of SBF (buffered with tris (hydroxymethyl) aminomethane (50 mM); and set at pH 7.2 with 1.0 N hydrochloric acid (HCl) [17])

Component	Concentration (mM)
Na^+	142.0
K^+	5.0
Ca^{2+}	2.5
Mg^{2+}	1.5
Cl^-	147.8
$(HCO_3)^-$	4.2
$(HPO_4)^{2-}$	1.0
$(SO_4)^{2-}$	0.5

After rinsing in distilled water and drying at room temperature, the specimens were characterized by XRD, FTIR spectroscopy, SEM and EDS.

2.3. Scratch testing

Scratch testing was performed using a Revetest automatic scratch tester (Centre Suisse d'Electronique et de Microtechnique) with a Rockwell C diamond stylus (conical angle, 120°; hemispherical tip, 200 μm). A scratch was performed under linearly increasing load from 1 to 30 N and with a specimen traversal rate at 10 mm min^{-1}. The mode of coating loss was studied in all cases by reflected-light microscopy. The critical load was taken as the onset of coating loss whether by flaking or by massive loss in the scratch channel.

3. Results

3.1. Physicochemical analysis

Figs 1 and 2 show the calcium and phosphate concentrations respectively, of the different calcium phosphate coatings in SBF buffer during the 4 weeks' incubation period.

For the amorphous coatings, we observed that the CaP-0.1 coatings after incubation for 2 weeks had dissolved completely. The CaP-1 coating showed an increase in Ca and P concentrations up to 3 weeks' incubation; then the Ca and P concentration started to decrease. Finally, for the CaP-4 coatings, increases in the Ca and P concentration was found only during the incubation period.

In contrast with the amorphous specimens, all heat-treated coatings dissolved only slightly within the first week. Then the Ca and P concentrations decreased and stabilized around the ion concentration of the SBF dissolution.

XRD measurements confirmed that after 4 weeks' incubation the amorphous CaP-0.1 and CaP-1 coatings had disappeared and that only the CaP-4 could be detected (Fig. 3, curve (a)). XRD evaluation of the heat-treated coatings confirmed their presence still after 4 weeks' incubation. In addition, the appearance of these patterns was not changed compared with pre-incubation (Fig. 3, curve b, Fig. 4 and Fig. 5).

FTIR spectra demonstrated that the amorphous CaP-0.1 and CaP-1 coatings had also disappeared.

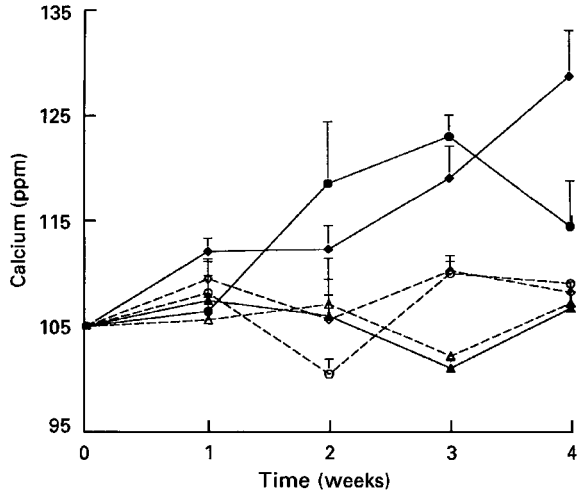

Figure 1 Graph showing the calcium release of various magnetron-sputtered Ca–P coatings ((—▲—), CaP-0.1; (—●—), CaP-1; (—◆—), CaP-4)) in Gomori's solution with pH 7.2 at 37 °C and for these coatings with an additional heat treatment for 2 h at 500 °C ((---△---), CaP-0.1, heat treated; (---⊙---), CaP-1, heat treated; (---◇---), CaP-4, heat treated).

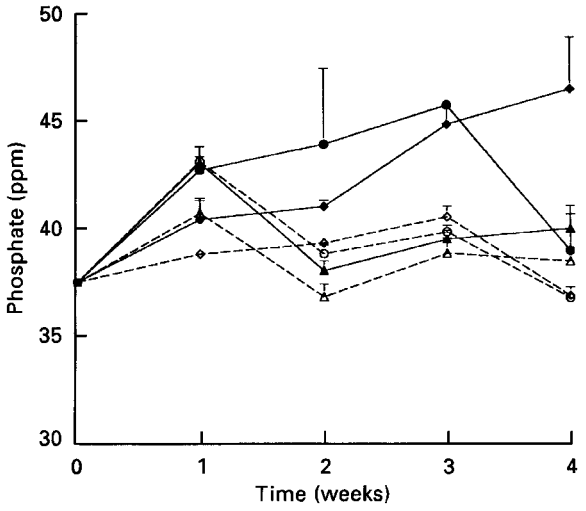

Figure 2 Graph showing the phosphate release of various magnetron-sputtered Ca–P coatings ((—▲—), CaP-0.1; (—●—), CaP-1; (—◆—), CaP-4)) in Gomori's solution with pH 7.2 at 37 °C and for these coatings with an additional heat treatment for 2 h at 500 °C ((---△---), CaP-0.1, heat treated; (---⊙---), CaP-1, heat treated; (---◇---), CaP-4, heat treated.

The amorphous CaP-4 coatings still showed, similar to the as-sputtered coatings, the presence of broad phosphate bonds in the regions at 1000 and 600 cm^{-1} (Fig. 6). The same was true for the heat-treated samples; on all the tested specimens PO bonds were found similar to the as-sputtered coatings (Fig. 7).

SEM and EDS evaluation agreed with the other measurements. After 4 weeks' incubation the amorphous CaP-4 coatings showed signs of surface dissolution and, besides a gradual decrease in thickness, also locations with a more severe dissolution (Fig. 8). As demonstrated by EDS, the amorphous CaP-0.1 and CaP-1 coatings had completely disappeared at 4 weeks. All heat-treated coatings appeared to be present even after 4 weeks' incubation. Occasionally,

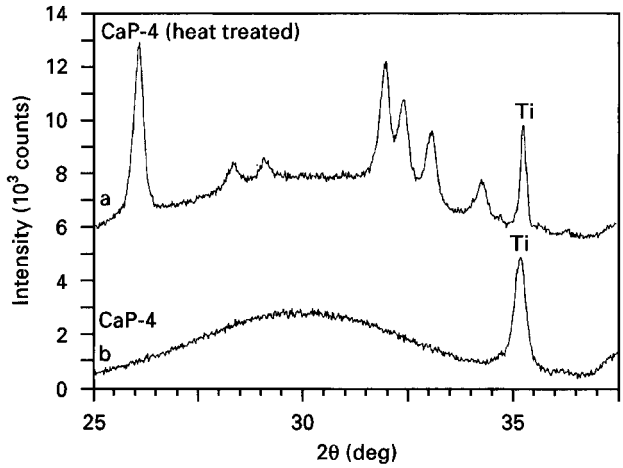

Figure 3 X-ray diffraction patterns of amorphous CaP-4 coating (curve a) and heat-treated CaP-4 coating (curve b) after 4 weeks' incubation, showing an amorphous – crystalline structure.

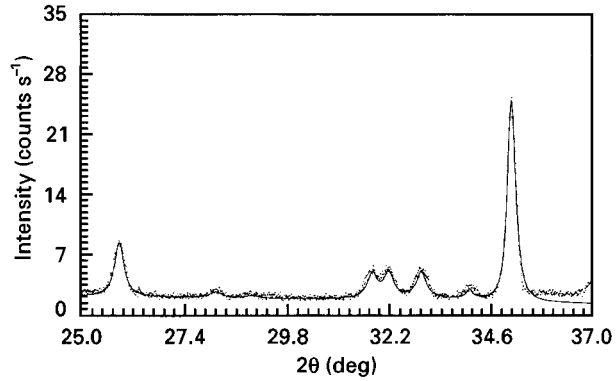

Figure 4 A thin-film X-ray diffraction pattern of a heat-treated CaP-0.1 coating showing an amorphous – crystalline structure.

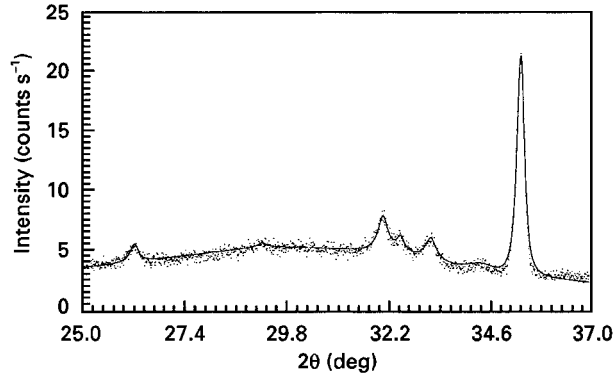

Figure 5 A thin-film X-ray diffraction pattern of a heat-treated CaP-1 coating showing an amorphous – crystalline structure.

these coatings showed signs of local dissolution and at these sites a granular precipitate was deposited (Fig. 9). EDS examination revealed that the Ca-to-P ratio of this precipitate varied between 1.6 and 1.75. Further, we observed that the heat-treated coatings still had the same crackled surface appearance as before the incubation (Fig. 10).

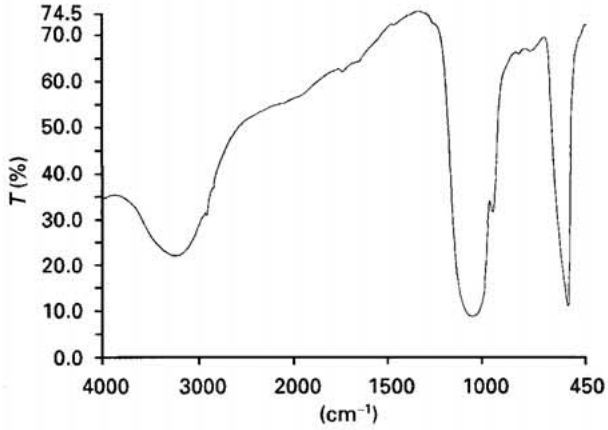

Figure 6 FTIR spectrum of the amorphous CaP-4 coating after 4 weeks' incubation.

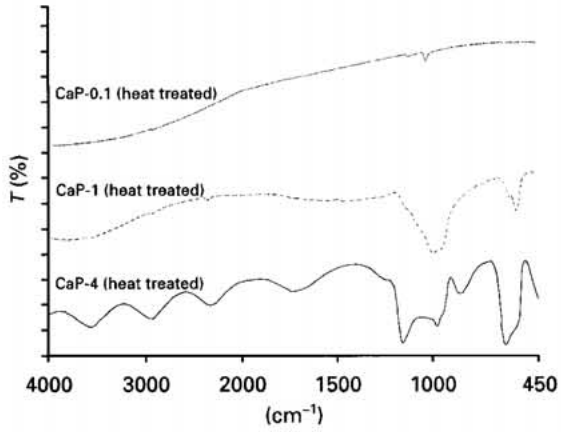

Figure 7 FTIR spectrum of the heat-treated specimens after 4 weeks' incubation.

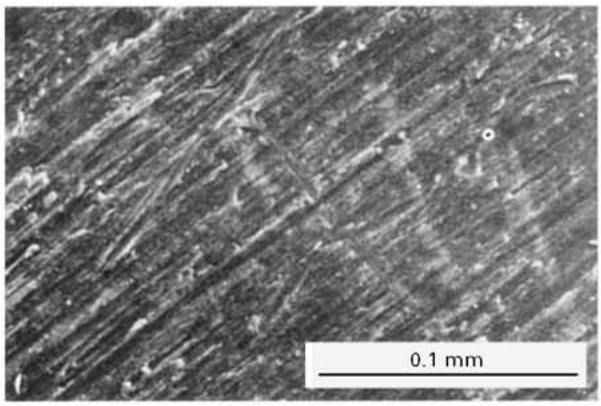

Figure 8 Scanning electron micrograph of an amorphous CaP-4 coating after 4 weeks' incubation. The coated surface showed some surface dissolution.

3.2. Scratch testing

The results of the scratch test performed on the coated samples are presented in Table II. The critical load, L_c, represents the mean value of three scratches for the cohesive failure (spallation) of the Ca–P coatings. Statistical testing of the results, using a one-way analysis of variance (ANOVA) and a multiple Tukey comparison procedure, showed a significant difference ($p \leqslant 0.05$) for the amorphous Ca–P coatings compared with all heat-treated Ca–P coatings. Further, using a simple linear regression test proved the existence of a strong correlation ($r = 0.97$ for the amorphous coatings, and $r = 0.99$ for the heat-treated coatings) between the coating thickness and critical load.

Light microscopy evaluation of the amorphous coatings showed only cohesive failure with cracks leading to adhesion failure with spallation on either side of the scratch trace (Fig. 11). A further increase in

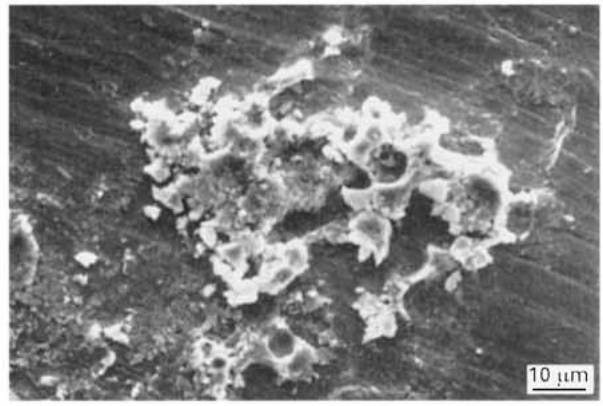

Figure 9 Scanning electron micrograph of a heat-treated CaP-0.1 coating after 4 weeks' incubation. The coated surface showed signs of local dissolution and a granular Ca–P precipitate was formed.

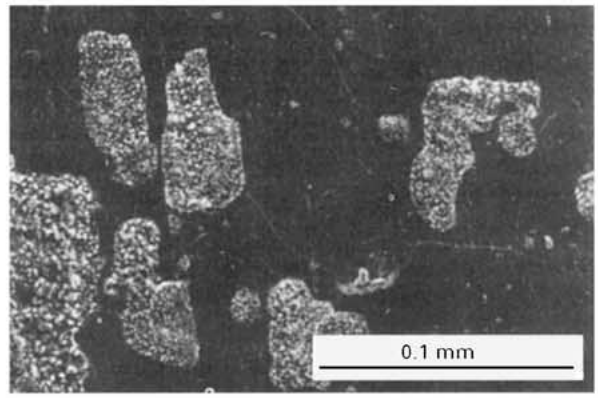

Figure 10 Scanning electron micrograph of a heat-treated CaP-4 coating after 4 weeks' incubation. The coated surface showed in addition to the deposition of a precipitate the formation of some cracks, due to the heat treatment procedure.

TABLE II Critical load values for Ca–P coatings with different thicknesses and an additional heat treatment for 2 h at 500 °C

Coating	Coating thickness (μm)	Critical load, L_c (N)	Standard deviation (N)
CaP-0.1	0.1	15.70	0.46
CaP-0.1 (heat treated)	0.1	13.77	0.45
CaP-1	1.0	12.03	0.45
CaP-1 (heat treated)	1.0	10.50	0.50
CaP-4	4.0	6.37	1.27
CaP-4 (heat treated)	4.0	1.60	0.56

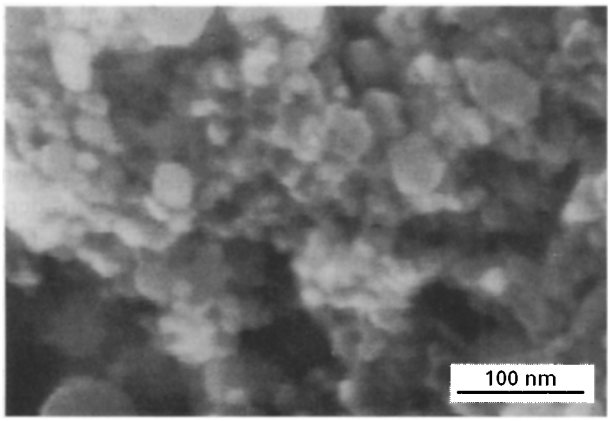

Figure 2 Scanning electron micrograph showing nanocrystalline silver particles synthesized from silver nitrate solution by the laser–liquid interaction.

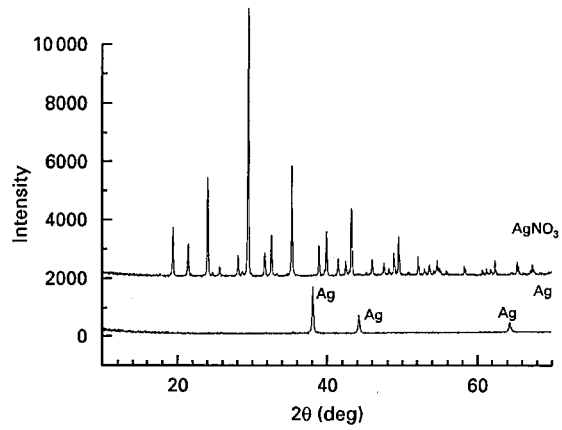

Figure 3 X-ray diffraction analysis showing pure silver particles recovered from silver nitrate solution.

formation) and nitrogen. Thus, high-quality silver nano particles were formed by this novel laser–liquid interaction technique.

Fig. 5 shows a scanning electron micrograph of the nanocrystalline silver particles produced from the silver nitrate solution using a focussed CW CO_2 laser-beam at a power of 300 W and an exposure time of 3 min. Relatively large nanospherical particles were synthesized in the size range from 100–1000 nm. In addition, agglomerated nanoparticles have also been found under these conditions.

Fig. 6 shows a scanning electron micrograph of the silver particles produced at a beam–powder of 300 W and a longer exposure time of 7 min. The major portion of the nanoparticles produced is an agglomerated mass along with some spherical particles of size 100–1000 nm. This can be explained by the fact that a higher exposure time resulted in the interaction of the laser beam with the nanoparticles, which caused agglomeration.

Fig. 7 shows a scanning electron micrograph of the nanocrystalline silver particles formed by this technique using the CO_2 laser beam at a power of 400 W, a defocused beam diameter of 3 mm and an exposure time of 3 min. Recirculation of the solution has been used to produce these powder particles.

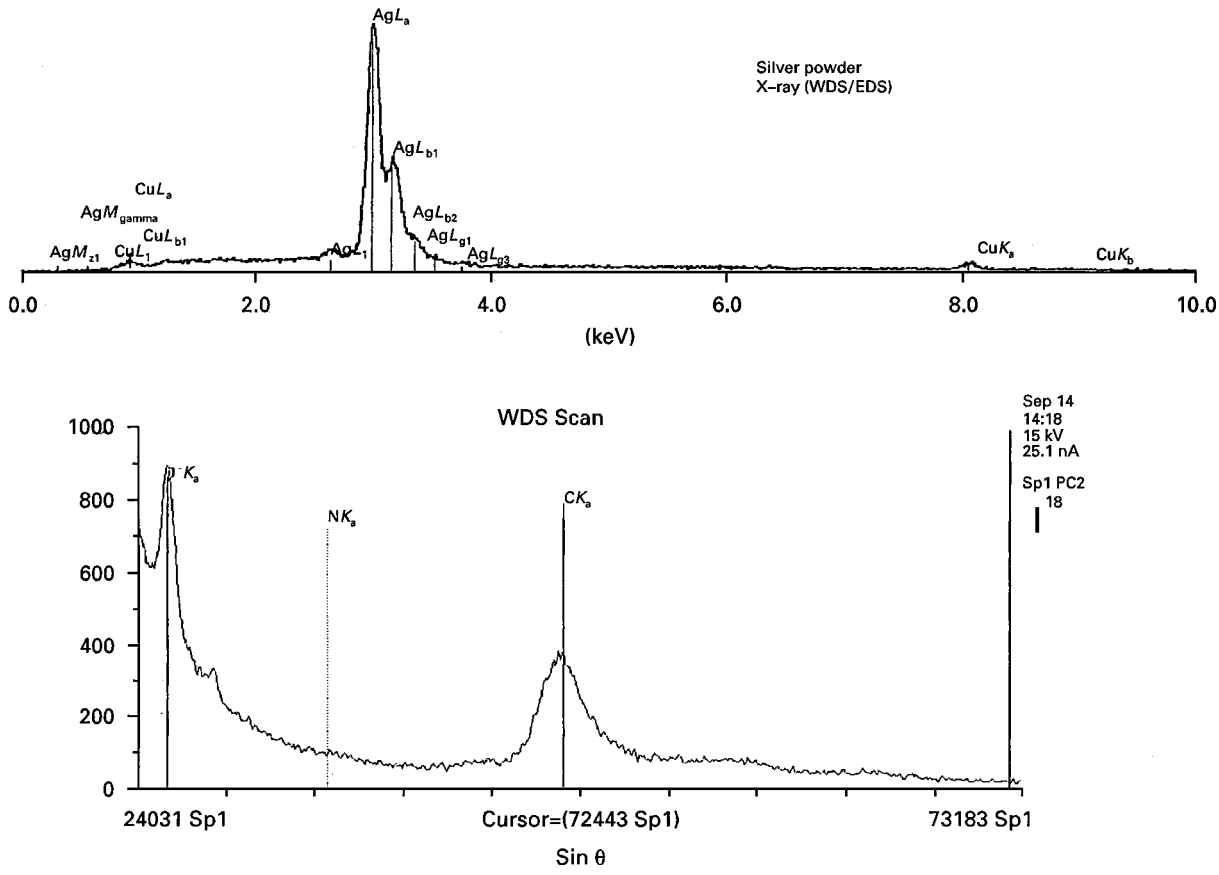

Figure 4 Energy dispersive X-ray microchemical data obtained from the silver particles in the electron microprobe.

Mr W. Molleman (Laboratory for Crystallography, University of Amsterdam, The Netherlands) for the thin-film XRD.

References

1. R. D. BLOEBAUM and J. A. DUPONT, *J. Arthropl.* **8** (1993) 195.
2. J. A. M. CLEMENS, Thesis, University of Leiden, Leiden (1995).
3. F. J. KUMMER and W. L. JAFFE, *J. Appl. Mater.* **3** (1992) 211.
4. P. FRAYSSINET D. HARDY, J. S. HANKER and B. L. GIAMMARA, *Cell Mater.* **5** (1995) 125.
5. W. R. LACEFIELD, *Ann. NY Acad. Sci.* **523** (1988) 72.
6. J. A. JANSEN, J. G. C. WOLKE, S. SWANN, J. P. C. M. VAN DER WAERDEN and K. DE GROOT, *Clin. Oral. Impl. Res.* **4** (1993) 28.
7. J. G. C. WOLKE, K. VAN DIJK, H. G. SCHAEKEN, K. DE GROOT and J. A. JANSEN, *J. Biomed. Mater. Res.* **28** (1994) 1477.
8. C. P. A. T. KLEIN, P. PATKA, H. B. M. VAN DER LUBBE, J. G. C. WOLKE and K. DE GROOT, *ibid.* **25** (1991) 53.
9. W. J. A. DHERT, C. P. A. T. KLEIN, J. G. C. WOLKE, E. A. VAN DER VELDE, K. DE GROOT and P. M. ROZING, *ibid.* **25** (1991) 1183.
10. J. G. C. WOLKE, K. DE GROOT and J. A. JANSEN, *ibid.* **39** (1998) 524.
11. P. LI, Thesis, University of Leiden, Leiden (1993).
12. J. L. VOSSEN, in "Adhesion measurement of thin films, thick films, and bulk coatings" (ASTM Special Technical Publication 640, edited by K. L. Mittal, American Society for Testing and Materials, Philadelphia, PA, 1978) p. 122.
13. S. KRONGELB, in "Adhesion measurement of thin films, thick films, and bulk coatings" (ASTM Special Technical Publication 640, edited by K. L. Mittal, American Society for Testing and Materials, Philadelphia, PA, 1978) p. 107.
14. P. R. CHALKER, S. J. BULL and D. S. RICKERBY, *Mater. Sci. Engng.* **A140** (1991) 583.
15. P. J. BURNETT and D. S. RICKERBY, *Thin Solid Films* **157** (1988) 233.
16. P. A. STEINMAN, Y. TARDY and H. E. HINTERMANN, *ibid.* **154** (1987) 333.
17. P. LI, C. OHTSUKI, T. KOKUBO, K. NAKANISHI, N. SOGA, T. NAKAMURA and T. YAMAMURO, *J. Appl. Biom.* **4** (1993) 221.
18. J. G. C. WOLKE, K. DE GROOT and J. A. JANSEN, *Biomaterials* **18** (1998) 483.
19. A. W. EBERHARDT, B. S. KIM, E. D. RIGNEY, G. L. KUTNER and C. R. HARTE, *J. Appl. Biom.* **6** (1995) 171.
20. C. JULIA-SCHMUTZ and H. E. HINTERMAN, *Surf. Coat. Technol.* **48** (1991) 1.
21. J. E. PAWEL and C. J. MCHARGUE, *J. Adhes. Sci. Technol.* **2** (1988) 369.

Received 27 January 1997
and accepted 18 March 1998